Experimental Neurology 348 (2022) 113923

Contents lists available at ScienceDirect

Experimental Neurology

journal homepage: www.elsevier.com/locate/yexnr

Research paper

Preclinical investigation of Pegylated arginase 1 as a treatment for retina and brain injury

Abdelrahman Y. Fouda [a,b,1,*], Wael Eldahshan [c,1], Zhimin Xu [c,d], Tahira Lemtalsi [c,d], Esraa Shosha [b,c], Syed AH. Zaidi [c,d], Ammar A. Abdelrahman [b,d,e], Paul Ning-Man Cheng [h], S. Priya Narayanan [c,d,f,g,i], R. William Caldwell [d,e], Ruth B. Caldwell [c,d,f,g,*]

[a] Department of Pharmacology and Toxicology, University of Arkansas for Medical Sciences, Little Rock, AR, USA
[b] Department of Clinical Pharmacy, Faculty of Pharmacy, Cairo University, Cairo, Egypt
[c] Vascular Biology Center, Augusta University, Augusta, GA, USA
[d] Culver Vision Discovery Institute, Augusta University, Augusta, GA, USA
[e] Department of Pharmacology and Toxicology, Augusta University, Augusta, GA, USA
[f] Department of Cellular Biology & Anatomy, Augusta University, Augusta, GA, USA
[g] Charlie Norwood VA Medical Center, Augusta, GA, USA
[h] Bio-cancer Treatment International, 511-513, Bioinformatics Building, Hong Kong Science Park, Tai Po, Hong Kong, China
[i] Department of Clinical and Administrative Pharmacy, University of Georgia, Augusta, GA, United States

ARTICLE INFO

Keywords:
Retinal ischemia
Stroke
Ischemia-reperfusion injury
Neuroprotection
Neurodegeneration
Arginase

ABSTRACT

Arginase 1 (A1) is the enzyme that hydrolyzes the amino acid, L-arginine, to ornithine and urea. We have previously shown that A1 deletion worsens retinal ischemic injury, suggesting a protective role of A1. In this translational study, we aimed to study the utility of systemic pegylated A1 (PEG-A1, recombinant human arginase linked to polyethylene glycol) treatment in mouse models of acute retinal and brain injury. Cohorts of WT mice were subjected to retinal ischemia-reperfusion (IR) injury, traumatic optic neuropathy (TON) or brain cerebral ischemia via middle cerebral artery occlusion (MCAO) and treated with intraperitoneal injections of PEG-A1 or vehicle (PEG only). Drug penetration into retina and brain tissues was measured by western blotting and immunolabeling for PEG. Neuroprotection was measured in a blinded fashion by quantitation of NeuN (neuronal marker) immunolabeling of retina flat-mounts and brain infarct area using triphenyl tetrazolium chloride (TTC) staining. Furthermore, ex vivo retina explants and in vitro retina neuron cultures were subjected to oxygen-glucose deprivation (OGD) followed by reoxygenation (R) and treated with PEG-A1. PEG-A1 given systemically did not cross the intact blood-retina/brain barriers in sham controls but reached the retina and brain after injury. PEG-A1 provided neuroprotection after retinal IR injury, TON and cerebral ischemia. PEG-A1 treatment was also neuroprotective in retina explants subjected to OGD/R but did not improve survival in retinal neuronal cultures exposed to OGD/R. In summary, systemic PEG-A1 administration is neuroprotective and provides an excellent route to deliver the drug to the retina and the brain after acute injury.

1. Introduction

Many neurodegenerative disorders involve a phase of ischemia or discontinuation of the blood supply. In the brain, this can manifest in the form of strokes and in the retina it can happen in different conditions that are collectively termed ischemic retinopathies. Examples of ischemic retinopathies include diabetic retinopathy, glaucoma, retinopathy of prematurity, and retinal artery or vein occlusion. Stroke is a leading cause of morbidity and mortality while ischemia-induced retinopathy is a leading cause of blindness and disability. While there are treatments and interventions for these ischemic conditions, they are often limited by the side effects, exclusion criteria or narrow time window making them not applicable for every patient. Therefore, there is a strong need for safe and effective treatments that can protect neurons

* Corresponding authors at: Department of Pharmacology and Toxicology, 4301 West Markham Street, University of Arkansas for Medical Sciences, Little Rock, AR, 72205, USA; Vascular Biology Center, 1460 Laney Walker Blvd, Augusta University, Augusta, GA 30912-2500, USA.
E-mail addresses: afouda@uams.edu (A.Y. Fouda), rcaldwel@augusta.edu (R.B. Caldwell).
[1] Equal contribution.

https://doi.org/10.1016/j.expneurol.2021.113923
Received 28 May 2021; Received in revised form 12 October 2021; Accepted 8 November 2021
Available online 12 November 2021

against ischemia (Fouda et al., 2020a).

The retina is considered part of the CNS and develops from the brain tissue during embryogenesis. Both retina and brain are composed of neurons, vasculature and supporting glia and it is well appreciated that disease mechanisms in the brain can be extended to the retina and vice versa (Fouda et al., 2020a; London et al., 2013; Jindal, 2015). Testing new therapeutics in both retina and brain injury models is important to confirm the potential neuroprotective effect and provides valuable insights to researchers in both brain and retina scientific communities.

Arginase is the enzyme that converts L-arginine to urea and ornithine. Arginase has two isoforms, arginase 1 (A1) and arginase 2 (A2). While A2 plays a deleterious role in retinal ischemia, A1 is protective (Fouda et al., 2018a; Shosha et al., 2016). Our recent work using a mouse model of acute retinal ischemia has shown worsened outcomes in mice lacking A1. Furthermore, intravitreal injection of a stable (pegylated) form of A1 that was prepared in our lab showed neuroprotection in this model (Fouda et al., 2018a). An investigational drug, pegylated arginase 1 (PEG-A1, also called BCT-100), has been developed for treating cancers auxotrophic for L-arginine. It shows favorable pharmacokinetic and pharmacodynamic profiles and is currently under investigation in multiple preclinical cancer models as well as clinical trials (Morrow et al., 2013; Feun et al., 2015; Yau et al., 2015). We hypothesized that systemic delivery of PEG-A1 could have a strong therapeutic potential for retina and brain ischemic conditions. However, PEG-A1 is a hydrophilic drug and has been reported to exhibit poor central nervous system (CNS) penetration (De Santo et al., 2018). Therefore, we also investigated the possible penetration of PEG-A1 across the blood-brain and blood-retina barriers after injury.

In this report, we demonstrate the protective effect of systemic PEG-A1 administration in mouse models of ischemic stroke, retinal ischemia-reperfusion (IR) injury, traumatic optic neuropathy (TON) as well as ex vivo in retinas subjected to oxygen-glucose deprivation / reoxygenation injury (OGD/R). Furthermore, PEG-A1 was detectable in the retina and brain tissues after injury and blood-retina/brain barrier breakdown but not after sham manipulation.

2. Materials and methods

2.1. Mouse retinal ischemia-reperfusion (IR) injury and optic nerve crush (ONC) models

All experiments were performed in accordance with the ARVO Statement for the Use of Animals in Ophthalmic and Vision Research and were approved by the institutional animal care and use committee (Animal Welfare Assurance no. D16-00197). Wild-type (WT) C57BL/6 J mice (10–12 weeks old) were anesthetized using ketamine/xylazine mixture then subjected to retinal ischemia-reperfusion (IR) injury or optic nerve crush (ONC) to model traumatic optic neuropathy (TON) as previously described (Shosha et al., 2016; Xu et al., 2018). Mice were sacrificed at 24 h or 7 days after by deep anesthesia followed by transcardial perfusion with PBS or thoracotomy. Eyeballs were then collected and fixed in 4% PFA for immunolabeling or retinas were extracted without fixation and homogenized in Radioimmunoprecipitation Assay (RIPA) lysis buffer for Western blotting.

2.1.1. IR-injury model

For induction of retinal IR-injury, mice were anesthetized with ketamine/xylazine mixture and a needle connected to an elevated saline reservoir was inserted into the anterior chamber the right eye to raise the intraocular pressure to 110 mmHg for 1 h. The left eye served as sham control.

2.1.2. ONC model

For induction of ONC, mice were anesthetized under isoflurane inhalation and one drop of topical anesthesia (0.5% proparacaine hydrochloride) was applied to the eyeball. The conjunctiva on the left eye was incised on the temporal side, and the orbital muscles were gently deflected while clamping (crushing) the optic nerve 1–2 mm from the eyeball for 3 seconds using a self-closing N7 forceps (Fine Science Tools, CA). The right eye was used as sham control.

2.2. MCAO model

C57BL/6 J mice (12–16 week-old male, 25–30 g) were subjected to middle cerebral artery occlusion (MCAO) using the intraluminal filament technique (Docol 602145) for 60-min followed by reperfusion as previously described (Eldahshan et al., 2019). A heating pad was used to maintain body temperature at 37 °C. Animals showed 12 to 14% weight loss at 24 h, which was not different between the groups. Testing was performed 1 h after reperfusion and animals that did not show a motor deficit after cerebral ischemia were excluded from the study. A total of nine animals out of 26 animals (34.6%) were excluded from study. Four animals were excluded immediately after reperfusion due to lack of deficit, and five animals were excluded at sacrifice due to subarachnoid hemorrhage. Sham surgery involved all the regular surgery steps except the filament insertion. Mice were deeply anesthetized at 24 h and sacrificed by trans-cardial perfusion with PBS. Then brains were collected and sectioned for triphenyl tetrazolium chloride (TTC) staining or homogenized in RIPA lysis buffer for western blotting.

2.2.1. Sensorimotor assessment

Bederson score was conducted as described previously (Bieber et al., 2019). Briefly, Mice were scored based on the following five parameters: 0) no observable deficit; 1) forelimb flexion; 2) forelimb flexion and decreased resistance to lateral push; 3) circling; 4) circling and spinning around the cranial-caudal axis; and 5) no spontaneous movement.

2.2.2. Infarct size analysis

Brain infarct size was determined based on TTC staining of brain sections as previously described (Eldahshan et al., 2019). Each mouse brain was cut into four 2-mm-thick coronal sections using a brain matrix after excluding the olfactory bulb, and the cerebellum, then stained with TTC. Images of TTC-stained sections were analyzed in a blinded fashion using ImageJ software [National Institutes of Health (NIH)], and the infarct size was calculated with edema correction using the following formula: $100 \times$ [nonstroked $-$ (stroked $-$ infarct)]/nonstroked.

2.3. PEGylated arginase 1 (PEG-A1) treatment

A pharmaceutical grade of PEG-A1 was provided as a kind gift from Bio-Cancer Treatment International Limited (BCT, Hong Kong). PEG-A1 is a recombinant human arginase (rhArg) covalently attached to methoxy polyethylene glycol (mPEG-SPA; MW 5000) via succinamide propionic acid (SPA) linker to increase its stability and half-life in vivo (half-life = 3 days vs a few minutes for the native enzyme) (Cheng et al., 2007). Methoxy polyethylene glycol propionic acid (MW 5000 – Sigma, Catalog number 88908-1G-F) was used as vehicle control. Animals were injected intraperitoneally with a dose of 25 mg/kg of PEG-A1 or PEG without arginase (vehicle control) at 3 h after brain or retina injury and at day 4 for mice sacrificed at day 7. The dose was selected based on the published literature and preliminary dose response studies, and dosing interval was based on the PEG-A1 in vivo half-life of 3 days (Cheng et al., 2007; Hernandez et al., 2010).

The cerebral ischemia experiment involved behavioral scoring and manual quantification of the infarct size, and was conducted in a blinded fashion. The surgeon performing the surgery, behavioral analysis and infarct size analysis was provided with drug treatment (PEG-A1) and control vehicle (PEG) that are masked and coded. Mice were randomly assigned to the coded treatments and unmasking was performed after completion of experiment and analysis. Another cohort of mice was subjected to MCAO without treatment to compare its outcomes to the treatment groups.

2.4. Ex vivo explants

Retinal explants were prepared according to published protocols with modifications (Alarautalahti et al., 2019; Johnson and Martin, 2008). Mice were deeply anesthetized by ketamine/xylazine mixture and then killed by cervical dislocation. Retinal eyecups were gently dissected and immersed in ice-cold HBSS containing penicillin (100 U/ml) and streptomycin (100 μg/ml). Under a dissecting microscope, the retinas were gently removed and cut radially into four separate equal-sized petals. The retina petals were placed in cell culture inserts (12 mm diameter, 0.4 μm pore, Millipore) with the inner retina facing up. The inserts were placed in 24-well plate in Neurobasal A medium supplemented with 2% B27 (Invitrogen), 1% N2 (Invitrogen), 2 mM GlutaMAX (Invitrogen), penicillin (100 U/ml), and streptomycin (100 μg/ml). Plates were placed in a humidified 37 °C incubator with 5% CO_2. For OGD/R experiments, explants were placed in DMEM no glucose medium in a hypoxia chamber (ProOx 110, Biospherix, <1% O_2, 94% N_2, and 5% CO_2 at 37 °C) for the desired duration (1, 3, or 5 h) then switched back to Neurobasal A growth medium and reoxygenated in a regular incubator (95% air, 5% CO_2 at 37 °C) for the reminder of a total 24-h experiment (23, 21, or 19 h respectively) to model the ischemia-reperfusion injury. At the end of the experiment, explants were fixed in 4% PFA and processed for flat-mount staining.

2.5. Myeloid A1 KO mice

One experiment was conducted on explants isolated from myeloid A1 knock out (M-A1 KO) mice and floxed ($A1^{f/f}$) controls (both on C57BL/6 J background). To generate the M-A1 KO mice, we crossed mice expressing Cre under control of the myeloid lineage-specific promoter of the lysozyme 2 gene (Lyz2) (LysMcre, Jackson Labs stock No. 004781) with $A1^{f/f}$ mice (Jackson Labs stock No. 008817). Genotype was determined by PCR using tail genomic DNA. The breeding, characterization, and confirmation of A1 deletion in these mice were described previously (Fouda et al., 2018a).

2.6. Western blotting

Western blotting on retina or brain was conducted as previously described (Fouda et al., 2018a). Membranes were probed with anti-PEG (RevMAb Biosciences, Cat # 31–1008-00, 1:1000), actin (Sigma, Cat # A5441), HSP90 (Stressgen, Cat # SPA-830) and anti-albumin (Bethyl Laboratories, 1:5000). Uncropped blots are included in Supplementary Fig. 1.

2.7. Fluorescent immunolabeling

Retinal flat-mounts were permeabilized and immunolabeled with anti-PEG antibody (RevMAb Biosciences, 1:400) and co-stained with Alex594-labeled Griffonia simplicifolia isolectin B4 (1:200; Invitrogen) as previously described (Shosha et al., 2016).

2.8. Evaluation of retinal neurodegeneration and microglia/macrophage count

2.8.1. Retinal neurodegeneration

Retina flat-mounts and explants were immunolabeled for the neuronal marker, NeuN (Millipore), as previously described (Shosha et al., 2016). *Z*-stack images were collected from the ganglion cell layer (GCL) to examine the surviving ganglion cells, which are mostly affected in the ischemic and traumatic injury models employed in this study. Four images per retina flat-mount were taken in the mid-periphery of each retina petal using an inverted confocal microscope (LSM 780; Carl Zeiss). Three images were taken per explant. Images were analyzed in a blinded fashion using a semi-automated method; NeuN-positive cells were quantified using ImageJ software (National Institutes of Health, Bethesda, MD). 'Batch processing' function was employed. A prerecorded ImageJ macrocode (Supplementary Fig. 2) was used for batch processing to create a *Z*-project for each stack of images using maximum intensity projection. The macro then creates an automatic thresholding followed by 'Analyze particles' function with size exclusion below 25 μm^2 to exclude non-specific speckles. The macro was validated every time it was used to make sure it is compatible with the set of images being analyzed. Results from four images per retina (three for explants) were averaged to represent neuron density for each retina. Results are presented as % surviving NeuN-positive cells in the GCL after injury as compared to sham retina or control explant under normoxia conditions.

2.8.2. Retinal microglia/macrophage count

Retina flat-mounts were immunolabeled for the microglia/macrophage marker, Iba-1 (Wako). *Z*-stack images were taken and the number of Iba-1 positive cells was quantified using the 'Analyze particles' function as described earlier.

2.9. Quantitative real time-PCR

RNA from the retina ($n = 5$/group) was isolated using RNAqueous-4PCR Total RNA Isolation Kit (Invitrogen, Carlsbad, CA, US) as per the manufacturer's instructions. 250 ng RNA was used to prepare cDNA using a high-capacity M-MLV reverse transcriptase (Invitrogen). RT-PCR was performed on cDNA (diluted 1 in 10 with nuclease-free water), using gene-specific primes on an ABI StepOne Plus Thermocycler (Applied Biosystems, Foster City, CA, US). The primers used in this study were either obtained from TaqMan gene expression assay (Applied Biosystems) or Integrated DNA Technologies (Coralville, IA, US). The details are provided in the Table below. The relative gene expression is calculated based on the comparative threshold cycle (ΔΔCt) method. Expression levels for all genes were normalized to the mean value of internal control, hypoxanthine phosphoribosyltransferase (HPRT), and reported as fold change to untreated controls.

Table of Primers used in the study:

Gene ID	Sequence / Reference ID	Probes	Source
MCP-1	Forward: GGCTCAGCCAGATGCAGTTAA Reverse: CCTACTCATTGGGATCATCTTGCT	SYBR Green	IDT
iNOS	Forward: GGCAGCCTGTGAGACCTTTG Reverse: TGCATTGGMGTGAAGCGTTT	SYBR Green	IDT
IL-10	Forward: GCTCTTACTGACTGGCATGAG Reverse: CGCAGCTCTAGGAGCATGTG	SYBR Green	IDT
IL-1β	Forward: TGCCACCTTTTGACAGTGATG Reverse: ATGTGCTGCTGCGAGATTTG	SYBR Green	IDT
F4/80	Forward: ATAGCTTCCGAGAGTGTTGTGGCA Reverse: TGTCTGACAATTGGGATCTGCCCT	SYBR Green	IDT
HPRT	Forward: GAAAGACTTGCTCGAGATGTCATG Reverse: CACACAGAGGGCCACAATGT	SYBR Green	IDT
TNF-α	Mm 00443258-m1	FAM	TaqMan Assay
BDNF	Mm 04230607-s1	FAM	TaqMan Assay
IL-6	Mm 00446190-m1	FAM	TaqMan Assay
A1	Mm00475988-m1	FAM	TaqMan Assay
HPRT	Mm00446968-m1	FAM	TaqMan Assay

2.10. Retinal neurons culture

2.10.1. Primary retinal neurons

Primary retinal mixed neurons were isolated from newborn Sprague-

Dawley (SD) rat pups at postnatal day (P) 1–2 as described previously with modifications (Perígolo-Vicente et al., 2014; Han et al., 2014). Retinas from ten pups were collected and washed twice with ice-cold 1 × PBS. They were digested with 0.5% trypsin for 3–4 min at 37 °C, followed by trypsin inactivation with the culture medium, DMEM/F12 (Gibco, Grand Island, NY) plus 10% FBS and 1% Penicillin-Streptomycin (P/S) solution (Invitrogen, Grand Island, NY). The retina tissue was mechanically dissociated by pipetting several times until cells were dispersed. Cells were then filtered through a 40 μm nylon-mesh filter, collected by centrifugation at 1000 rpm for 10 min, re-suspended in culture medium, and plated in 6 or 12 well-cell culture plates (Corning, Corning, NY) coated with Poly-D-lysine hydrobromide (PDL, Sigma) at a density of 0.5 × 106 cells / ml. The plates were maintained in a humidified CO2 incubator at 37 °C and 5% CO2. At days 1, 2, and 3 in vitro (DIV), half of the medium was aspirated and replaced with Neurobasal A medium containing 1× B-27 (GIBCO), 1× glutaMAX (GIBCO) and 1% P/S. Experiments were conducted at DIV 6. Immunofluorescence studies confirmed the high purity of cultured neurons using the neuron marker; Neuron-specific class III beta-tubulin (TuJ1), and glia marker; Glial fibrillary acidic protein (GFAP) (Supplementary Fig. 3).

2.10.2. R28 retinal neuronal-like cells

Cells were purchased from Kerafast, Inc. Boston, MA 02210. Cells were cultured and differentiated as described previously (Kong et al., 2016; Mathew et al., 2019; McLaughlin et al., 2018). Cell passages 67 to 70 were used for experiments. R28 cells were cultured in DMEM with low glucose (Sigma) supplemented with 10% FBS and 1% Penicillin-streptomycin, 1% Amphotericin B. For differentiation, cells were passaged into Laminin-coated plates and supplemented with 250 μM pCPT-cAMP for overnight incubation.

2.10.3. Oxygen-glucose deprivation/reoxygenation (OGD/R) protocol

Oxygen-glucose deprivation/reoxygenation (OGD/R) in vitro was used to mimic in vivo ischemia/reperfusion injury. To achieve OGD, neuron culture was incubated in a hypoxia chamber (ProOx 110, Biospherix, <1% O_2, 94% N_2, and 5% CO_2 at 37 °C) and glucose free DMEM medium and in some experiments this was followed by "reoxygenation" in complete medium under normoxic conditions (95% air, 5% CO_2 at 37 °C). Specific durations of OGD or OGD/R were as follows: Differentiated R28 cells were subjected to OGD for 3 or 24 h and treated with PEG-A1 (1 μg/ml) for the duration of experiment then LDH release assay (Roche) was conducted on the supernatant following the manufacturer's instructions. Another passage of R28 cells were exposed to 3 h of OGD followed by 3 h of reoxygenation and treated with PEG-A1 (0. 1 and 1 μg/ml) at reoxygenation followed by MTT (3-[4,5-dimethylthiazol-2-yl]-2,5 diphenyl tetrazolium bromide) assay as previously described (Jittiporn et al., 2014).

Primary retinal neurons were subjected to OGD for 6 h followed by reoxygenation for 18 h and treated with PEG-A1 (1 μg/ml) or the arginase inhibitor ABH (2(*S*)-amino-6-boronohexanoic acid, 100 μM) at reoxygenation followed by LDH release assay.

2.11. BMDMs

Bone marrow-derived macrophages (BMDMs) were freshly isolated from WT mice femurs and tibias and differentiated in culture using differentiation medium (DMEM high glucose containing 20% FBS, 20% L929 cells conditioned media, and 1% P/S) for 7 days as previously described (Fouda et al., 2018a). To determine PEG-A1 intracellular uptake by macrophages, BMDMs were treated overnight with PEG-A1 or vehicle in normal growth media (DMEM high glucose containing 20% FBS, and 1% P/S), and then washed several times with phosphate buffered saline (PBS) before collection in RIPA buffer for Western blotting.

2.12. Statistical analysis

Statistical analysis was conducted using GraphPad Prism 9 software. Differences between two groups were determined by student's *t*-test. Comparisons between multiple groups (retina explants and neuron culture experiments) were analyzed by ANOVA with Tukey's post-hoc test. *P* values <0.05 were considered as statistically significant. Graphs were prepared using GraphPad Prism 9 software and data were presented as mean ± standard error (SE).

3. Results

3.1. Systemic PEG-A1 treatment crosses the blood-retina barrier and provides neuroprotection after IR

Our previous work has shown a deleterious effect of A1 deletion in mouse model of acute retinal ischemic injury, thus suggesting a protective role of A1 (Fouda et al., 2018a). Here, we tested the utility of systemic PEG-A1 administration in the same model. To examine the PEG-A1 penetration of the blood-retina barrier with systemic treatment, mice were subjected to 1 h of unilateral retinal ischemia-reperfusion injury and injected with PEG-A1 (25 mg/kg, i.p.) at 3 h after reperfusion. Mice were deeply anesthetized and sacrificed 24 h later by transcardial perfusion with PBS (Fig. 1A). Western blotting showed a strong band for anti-PEG immunoreactivity in liver homogenates of PEG-A1 treated mice (Fig. 1B). Retina homogenates from the sham eyes of treated mice showed faint anti-PEG reactive bands while the IR-injured retinas from the same mice showed strong anti-PEG reactivity as well as increased levels of albumin leakage, a measure of the IR-induced increase in permeability of the blood-retinal barrier (Fig. 1C). Another cohort of WT mice were subjected to sham or IR injury and treated with PEG-A1 (25 mg/kg, i.p.) at 3 h after reperfusion and at day 4. These mice were sacrificed at day 7 without transcardial perfusion and retina flat-mounts were immunolabeled to show PEG distribution within the retina (Fig. 1D). In the sham retinas, the PEG signal was restricted to a vessel-like network. The IR-injured retinas showed a more diffuse signal, suggesting extravasation of PEG-A1 had occurred after the injury (Fig. 1E). Taken together, these results show an enhanced penetration of PEG-A1 after blood-retina barrier breakdown. Furthermore, mice treated with systemic PEG-A1 showed increased neuronal survival (62% vs 40% in the vehicle group) after retinal IR compared to the vehicle treated mice as measured by NeuN labeling of retinal flat-mounts at 7 days post-injury (Fig. 1F, G).

3.2. Systemic PEG-A1 treatment crosses the blood-brain barrier and provides neuroprotection after MCAO

We next evaluated the penetration of PEG-A1 into the brain and effect on outcomes after cerebral ischemia. WT mice were subjected to 60 min MCAO and treated with PEG-A1 or vehicle (PEG only) at reperfusion. Mice were sacrificed and transcardially perfused with PBS at 24 h after cerebral ischemia (Fig. 2A). Western blotting analysis showed a strong band of anti-PEG immunoreactivity in the stroked brains, which was also detectable with an anti-A1 antibody, thus confirming drug penetration to brain tissue after cerebral ischemia (Fig. 2B). To test the neuroprotective actions of PEG-A1 after cerebral ischemia, brain sections were stained with triphenyl tetrazolium chloride (TTC) for infarct analysis. Mice were also tested for behavioral deficit using Bederson score before sacrifice at 24 h. PEG-A1 treated mice showed significant reduction in infarct size (34 vs 41%) compared to vehicle treatment (Fig. 2C, D). Furthermore, PEG-A1 treated mice showed a trend towards improved Bederson score that did not reach statistical significance (Fig. 2E).

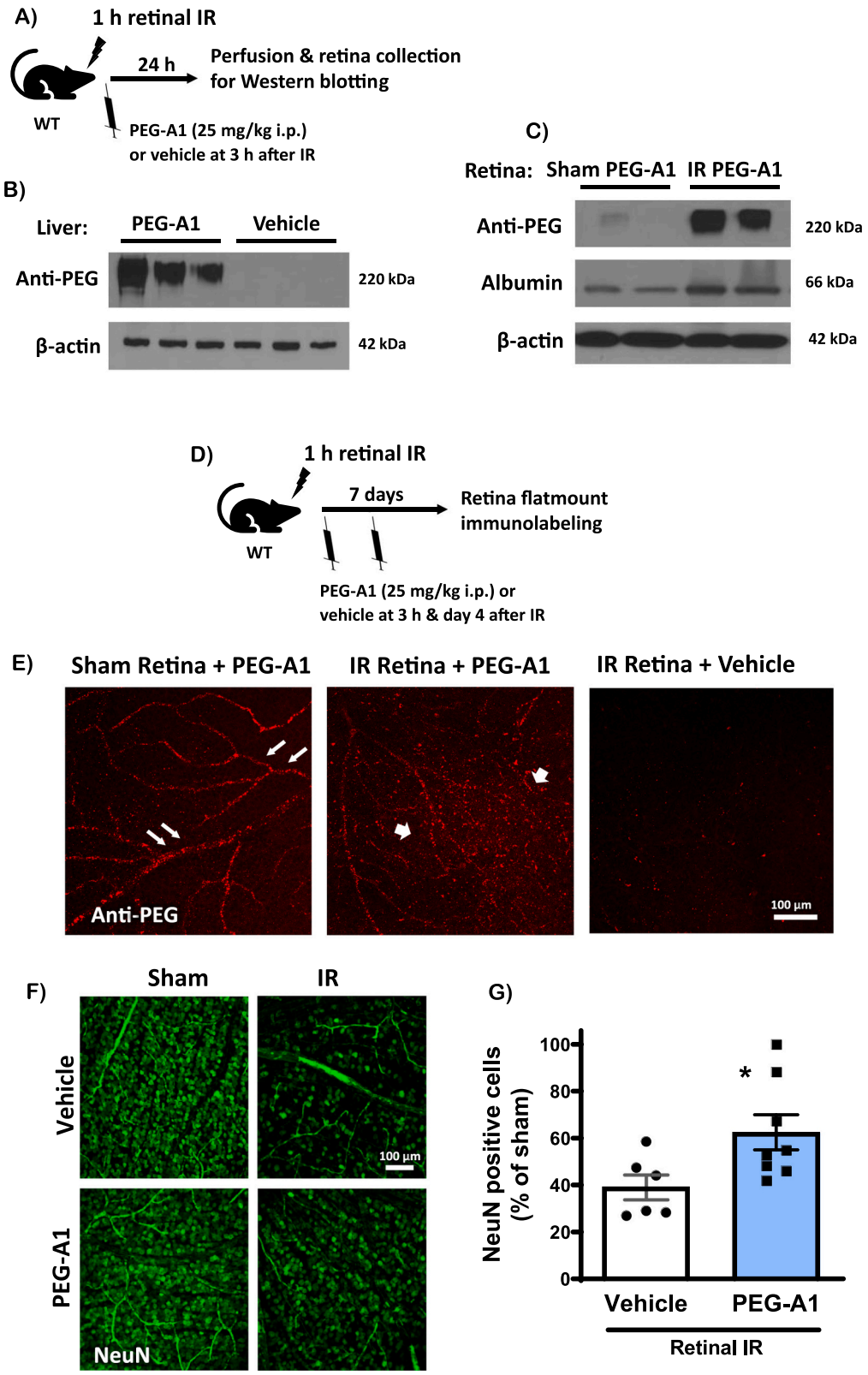

Fig. 1. Systemic PEG-A1 treatment is neuroprotective and crosses the blood-retina barrier after IR injury. A) Schematic representation of the experimental protocol for figs. B and C. B) PEG-A1 treated mice show a strong PEG-positive band in western blots of perfused liver homogenates collected at 24 h. C) Western blotting on perfused retinas collected at 24 h after treatment show a strong PEG positive band in the IR injured retinas but not the sham retinas from the same mice. IR injured retinas also show a stronger albumin band, an indicator of increased vascular permeability. D) Schematic representation of the experimental protocol for figs. E, F and G. E). Flat-mounts of retinas from PEG-A1 treated mice collected without perfusion at 7 days after treatment show an immunofluorescent signal that is confined to the retina vessel network in the sham eye with a more diffuse signal in the IR injured retinas. F, G) Neun staining and quantification of retina flat-mounts collected at 7 days after retinal IR show significant neuronal preservation after injury with PEG-A1 treatment as compared to vehicle treatment, $n = 6–8$, $^*p < 0.05$ vs vehicle group.

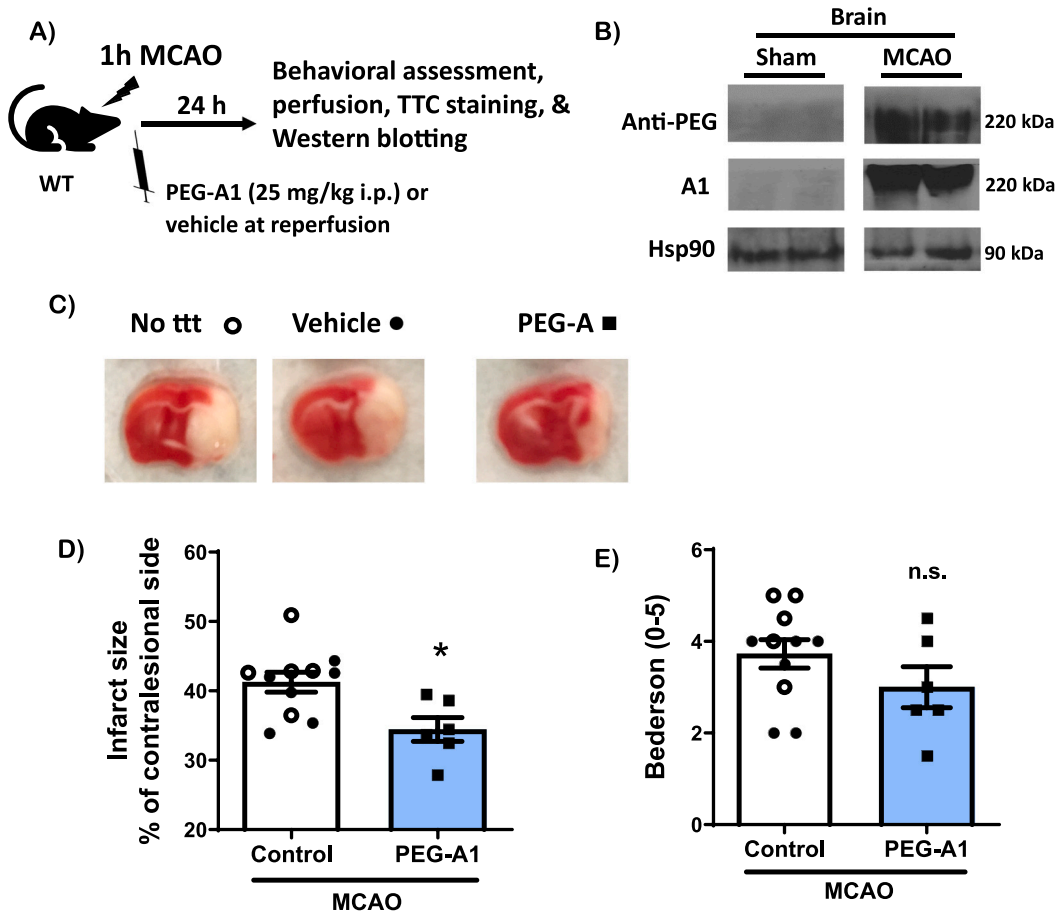

Fig. 2. Systemic PEG-A1 treatment is neuroprotective and crosses the blood-retina barrier after cerebral ischemia. A) Schematic representation of the experimental protocol for figs. B, C, D and E. B) Western blotting on perfused brain homogenates shows a strong band for anti-PEG after middle cerebral artery occlusion (MCAO) but not in the sham brains which is confirmed using anti-A1 antibody. C) Representative triphenyltetrazolium chloride (TTC) red staining of the viable tissue in brain tissue sections highlights the unstained infarct area in white color in mice with no treatment (ttt) and vehicle or PEG-A1 treated mice. D) Quantification of the infarct size as a percent of contralesional hemisphere shows significant reduction with PEG-A1 treatment (*$p < 0.05$ vs control). E) Bederson score of behavioral function after cerebral ischemia shows a trend towards improvement with PEG-A1 but the difference did not reach statistical significance. There was no difference in the infarct size or Bederson score between the untreated and the vehicle treated mice and therefore these groups were combined and identified by open and closed circles, respectively, n = 6–11, *$p < 0.05$ vs control group. (For interpretation of the references to color in this figure legend, the reader is referred to the web version of this article.)

3.3. Systemic PEG-A1 treatment crosses the blood-brain barrier and provides neuroprotection after ONC

We tested the effects of systemic PEG-A1 delivery in traumatic optic neuropathy (TON) using the optic nerve crush (ONC) model. Mice were subjected to ONC and treated with PEG-A1 three hours later At 24 h later the mice were sacrificed and perfused (Fig. 3A). Another group was given a booster dose at day 4 and then sacrificed without perfusion at day 7 (Fig. 3C). PEG-A1 showed effective penetration into the retina / optic nerve tissue homogenates but not into the brain or sham contralateral retina / optic nerve at 24 h after ONC as measured by western blotting (Fig. 3B) and flat-mount immunolabeling at 7 days (Fig. 3D). Retina flat-mounts collected at 7 days post-ONC showed significant neuroprotection (78 vs 62% in the vehicle group) as measured by NeuN labeling and quantification (Fig. 3E, F).

3.4. Systemic PEG-A1 treatment mitigates retinal inflammatory response after ONC

We further examined the effect of PEG-A1 treatment on the retinal inflammatory response after ONC. PEG-A1 treatment reduced the number of retinal Iba-1 positive microglia/macrophages at 4 days after injury (Fig. 4A-C). RT-PCR analysis at the same time point showed upregulation of the inflammatory cytokines, interleukin (IL-) 1β, tumor necrosis factor-α (TNF-α), monocyte chemoattractant protein 1 (MCP-1), as well as inducible nitric oxide synthase (iNOS) and the macrophage marker, F4/80. PEG-A1 reduced IL-1β, TNF-α, and F4/80 but the latter two did not reach statistical significance. PEG-A1 treatment increased the immunomodulatory cytokine, IL-6 and the anti-inflammatory cytokine, IL-10. Moreover, PEG-A1 increased the growth and survival factor, brain derived neurotrophic factor (BNDF) (Fig. 4D-K). We further examined the effect of PEG-A1 treatment on endogenous A1 expression. We did not detect change in A1 mRNA levels after systemic treatment in either ONC or MCAO models (Supplementary Fig. 4).

3.5. PEG-A1 provides neuroprotection ex vivo

After establishing the protective effects of systemic treatment with PEG-A1, we next examined the direct effect of PEG-A1 on retinal neuronal survival ex vivo. We mimicked the retinal IR model by subjecting retinal explants to oxygen-glucose deprivation / reperfusion (OGD/R) ex vivo (Fig. 5A). An OGD time-response experiment established 3 h of OGD / 21 h of reoxygenation to be optimal for studying retinal neurodegeneration ex vivo with about 60% neuronal survival as measured by NeuN flat-mount staining (Fig. 5B, C). To test the effect of A1 treatment, retina explants were subjected to 3 h of OGD then treated

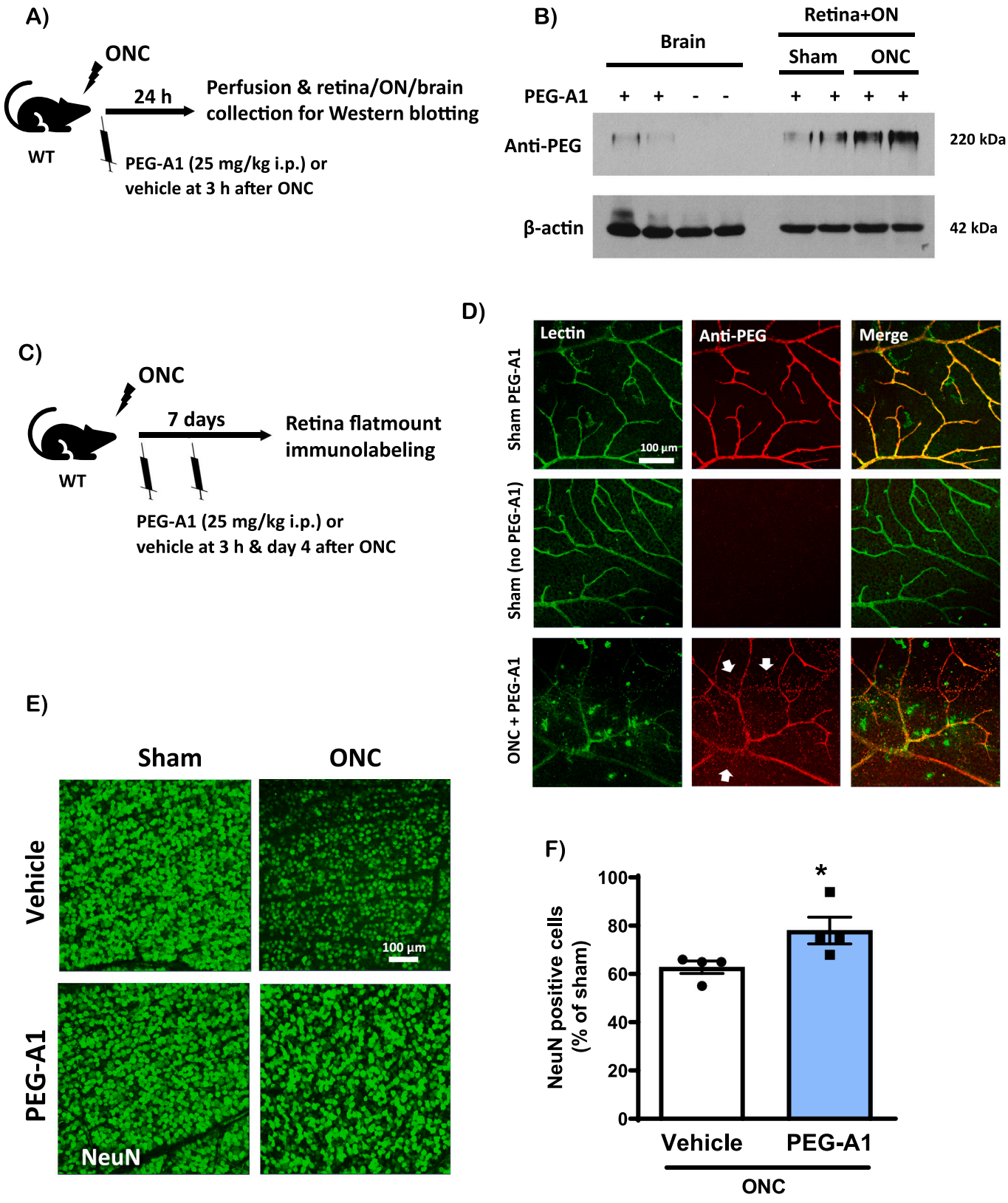

Fig. 3. Systemic PEG-A1 treatment is neuroprotective and crosses the blood-retina barrier after ONC. A) Schematic representation of the experimental protocol for fig. B. B) Western blotting on perfused retina and brain homogenates shows a strong band for anti-PEG in the retina/optic nerve (ON) subjected to ONC. Much less is present in brain or sham retina/ON which could be due to residual blood remaining after perfusion. C) Schematic representation of the experimental protocol for figs. D, E and F. D) Flat-mount immunolabeling using anti-PEG antibody and co-stained with lectin (stains vessels and some microglia/macrophages) shows PEG-A1 extravasation after ONC (white arrows). E, F) Flat-mount immunolabeling for the neuronal marker (NeuN) and quantification show significant neuronal preservation with PEG-A1 treatment after ONC, $n = 4$, $^*p < 0.05$ vs vehicle group.

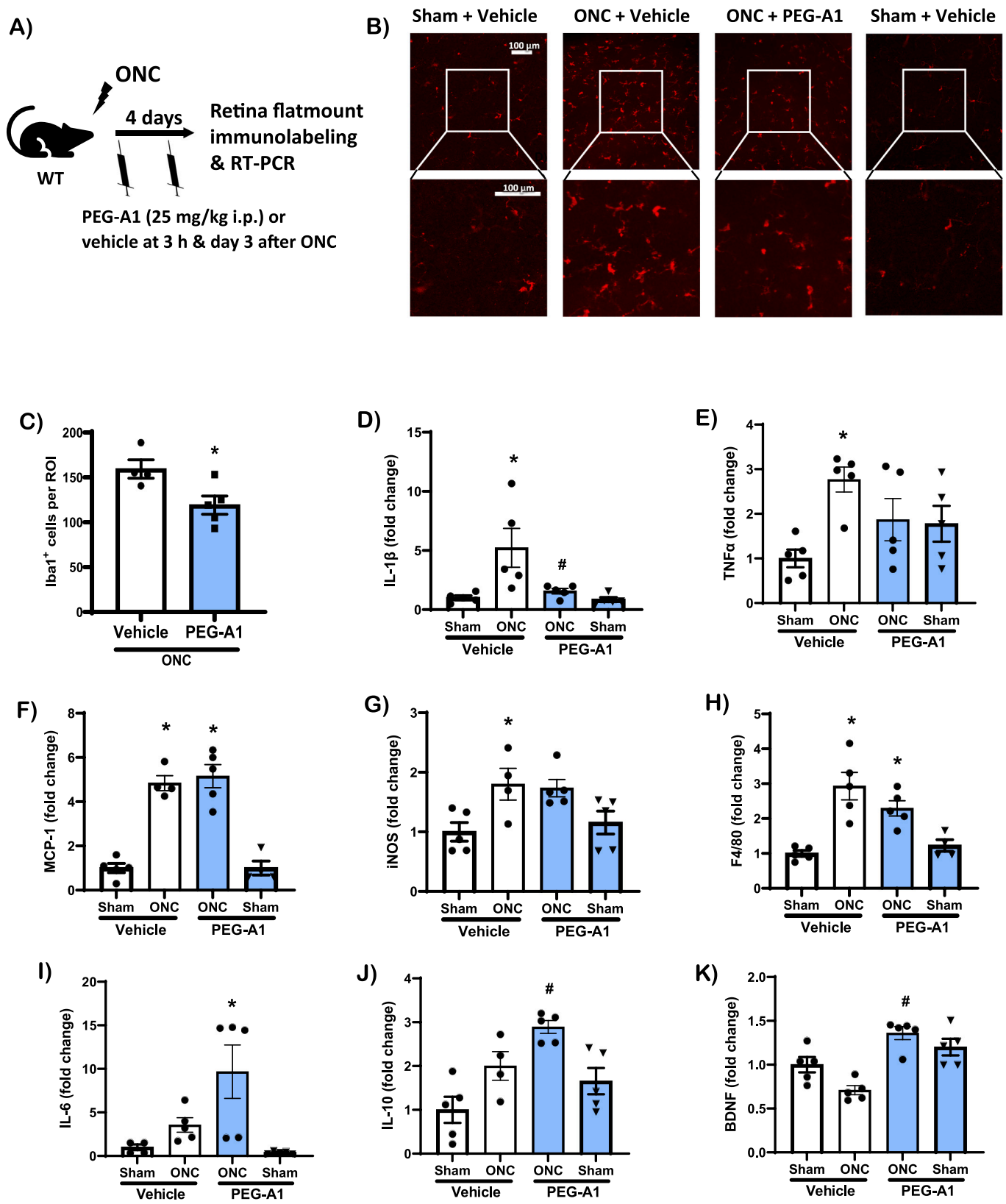

Fig. 4. PEG-A1 treatment mitigates retinal inflammatory response after ONC. A) Schematic representation of the experimental protocol for figs. B through K. B, C) Immunolabeling of retina flatmounts with the microglia/macrophage marker, Iba-1, and quantification showed a reduction in number with PEG-A1 treatment. n = 4–5, *$p < 0.05$ vs vehicle group. D—K) RT-PCR analysis of different cytokines at day 4 after ONC showed reduction in IL-1β, and increase in IL-6, IL-10 and BDNF with PEG-A1 treatment. n = 4–5, *p < 0.05 vs sham vehicle, #p < 0.05 vs ONC vehicle.

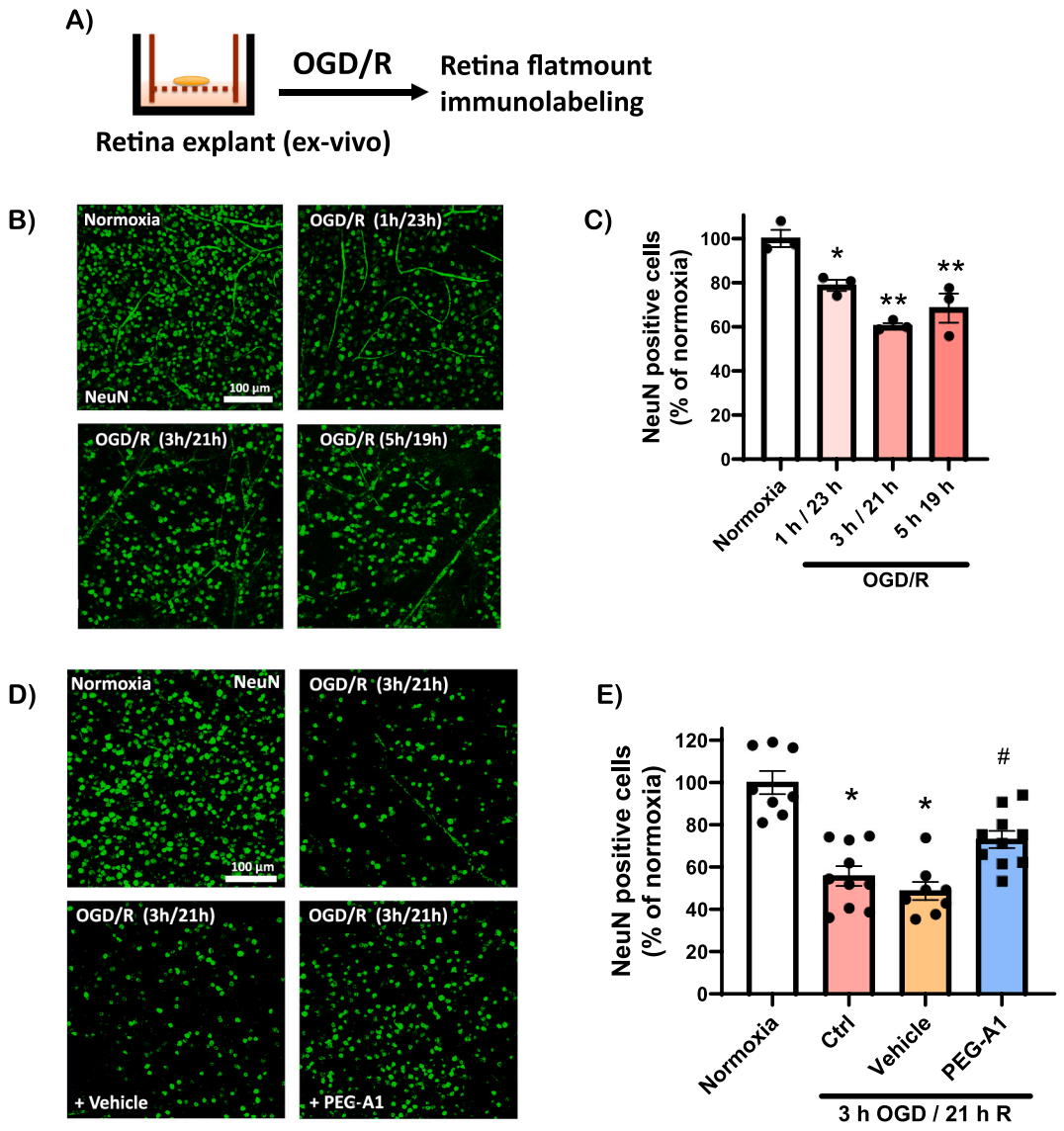

Fig. 5. PEG-A1 treatment protects retinal explants from oxygen-glucose deprivation/reoxygenation (OGD/R) injury ex vivo. A) Schematic representation of the experimental protocol for figs. B, C, D and E. B, C) Time course of exposing retina explants to OGD/R ex vivo followed by fixation and flat-mount immunolabeling with Neun showed neuronal degeneration after 1, 3 or 5 h of OGD then reoxygenation (R), with maximum neuronal loss (about 40%) after 3 h of OGD and 21 h of reoxygenation, $n = 3$ per group, $^{*}p < 0.05$ vs normoxia, $^{**}p < 0.01$ vs normoxia. D, E) PEG-A1 treatment at reoxygenation significantly protected the retina explant neurons against OGD/R (3 h/21 h) as compared to control (OGD/R without treatment) or vehicle treated (PEG only) explants, $n = 8$–10, $^{*}p < 0.05$ vs normoxia, $^{\#}p < 0.05$ vs OGD/R control and vehicle groups.

at reoxygenation with PEG-A1 (1 µg/ml) or control PEG. PEG-A1 treated explants showed significant neuronal preservation (73% survival) as compared to untreated or PEG only treated explants which showed 55 and 48% survival respectively (Fig. 5D, E).

3.6. PEG-A1 is not neuroprotective in vitro

To test the direct effect of PEG-A1 treatment in vitro we used retina neuron cultures subjected to different durations of OGD (Fig. 6A). R28 cells subjected to 6 or 24 h of OGD and treated with PEG-A1 (1 µg/ml) throughout the duration of experiment did not show any differences in cell death with or without treatment as measured by LDH release assay (Fig. 6B, C). Western blotting on R28 cell lysates confirmed the LDH release results with upregulation of the proapoptotic marker cleaved PARP after 6 h of OGD with no protective effect upon PEG-A1 treatment (Fig. 6D, E). Furthermore, R28 cells subjected to 3 h of OGD then 3 h of reoxygenation showed a 20% reduction in cell viability but there was no difference with or without PEG-A1 (0.1 and 1 µg/ml) treatment as measured by MTT assay (Fig. 6F). Finally, primary rat retinal mixed neurons subjected to 6 h of OGD and 18 h of reperfusion with PEG-A1 treatment showed increased cell death as measured by LDH release. Similarly, treatment with the arginase inhibitor, ABH (100 µM), led to a trend towards increased cell death, yet it did not reach statistical significance (Fig. 6G).

3.7. Retina explants from myeloid A1 KO mice show similar neurodegeneration to control mice subjected to oxygen-glucose deprivation reoxygenation (OGD/R) insult

We have previously shown that myeloid specific A1 deletion using the LysM cre mice leads to increased neurodegeneration in the retinal IR model. (Fouda et al., 2018a) However, our recent characterization of the LysM cre promoter showed a 10% neuronal recombination in the retina. (Fouda et al., 2020b) To test the effect of possible neuronal A1 deletion

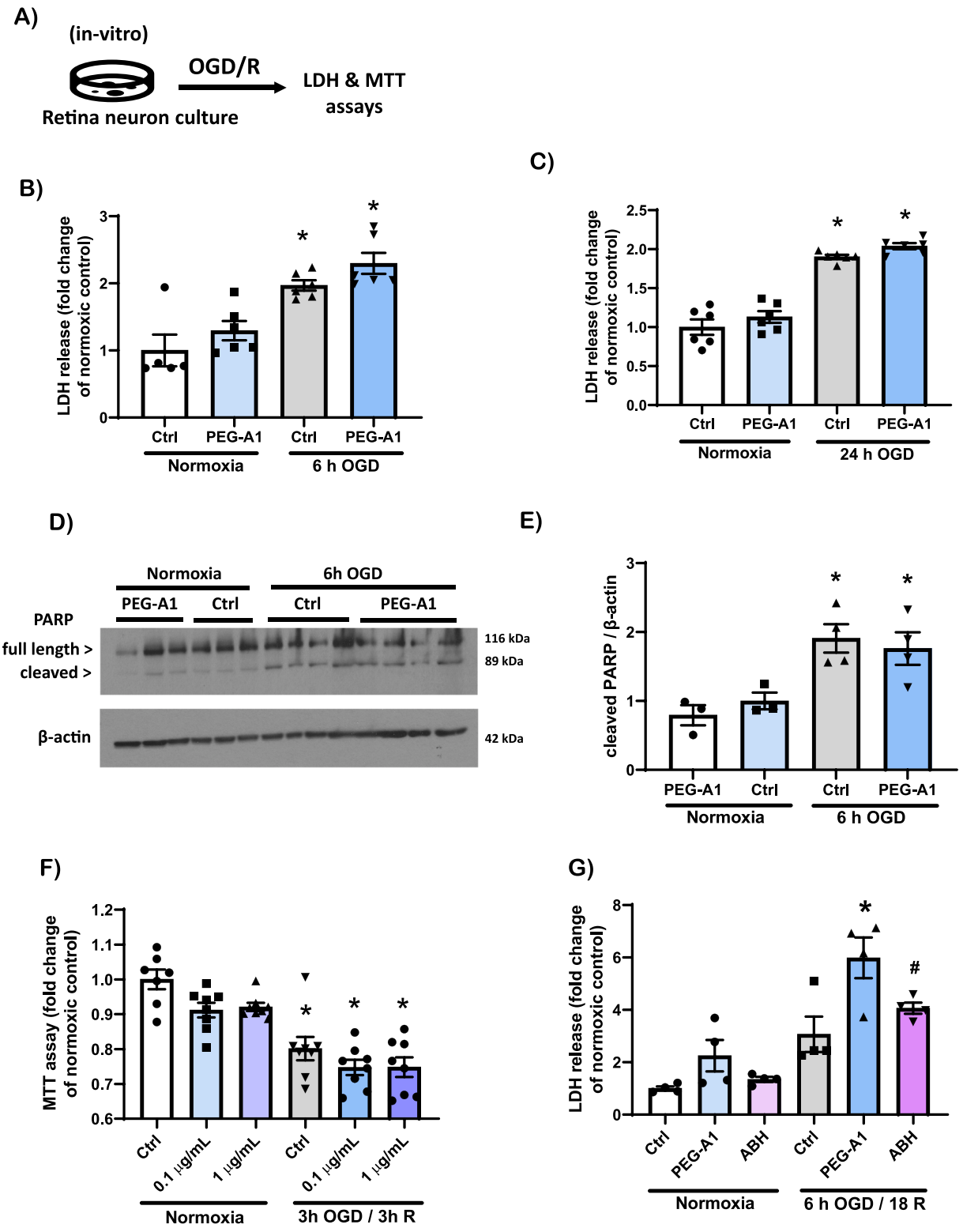

Fig. 6. PEG-A1 treatment does not provide neuroprotection to retinal neurons in vitro after OGD. A) Schematic representation of the experimental protocol for figs. B, C, D and E. B, C) R28 retinal neurons were subjected to OGD for 6 or 24 h with or without PEG-A1 treatment (1 μg/ml) followed by LDH release assay on the supernatant. OGD increased cell death as evident by a two-fold increase in LDH release while PEG-A1 did not alter this effect, *$p < 0.05$ vs control normoxia group. D, E) Western blotting on R28 cell lysates showed upregulation of cleaved PARP after 6 h of OGD which was not rescued by PEG-A1 treatment. F) MTT assay on R28 cells showed a 20% reduction in cell viability after 3 h of OGD and 3 h of reoxygenation while PEG-A1 treatment (0.1 or 1 μg/ml) did not show improvement in viability, *$p < 0.05$ vs control normoxia group. G) Primary rat retinal mixed neurons were subjected to OGD/R (6 h/18 h) and treated at reperfusion with PEG-A1 (1 μg/ml) or ABH (100 μM). Neither treatment with PEG-A1 or ABH promoted protection as measured by LDH release. *$p < 0.05$ vs control and PEG-A1 normoxia groups and ctrl OGD group, $^{\#}p < 0.05$ vs control and ABH normoxia groups.

on the previously reported IR outcome in these mice, we subjected control and myeloid-specific A1 KO retina explants to OGD/R (3 h / 21 h) (Fig. 7A). The explant model excludes any effects due to infiltrating myeloid cells. Neurodegeneration was not different between the two groups suggesting that the enhanced neurodegeneration in myeloid-specific A1 KO mice in vivo after IR is primarily due to lack of A1 in infiltrating myeloid cells (Fig. 7B, C). We have previously shown that PEG-A1 can mitigate the macrophage inflammatory response. To further test if macrophages can incorporate PEG-A1, we treated BMDMs with PEG-A1 or vehicle overnight and then washed them with PBS several times before Western blotting. Macrophage treated with PEG-A1 and analyzed by western blotting using anti-PEG antibody showed a strong band in cell lysate, thus suggesting that intracellular uptake of PEG-A1 had occurred (Fig. 7D).

4. Discussion

This report shows for the first time the neuroprotective effect of systemic PEG-A1 administration after cerebral ischemia, retinal IR-injury and traumatic optic neuropathy (TON). Furthermore, PEG-A1 given systemically was able to cross the blood-brain and blood-retina barriers after acute brain or retina injury, respectively.

The role of arginase in acute retina and brain injury has been recently reviewed (Fouda et al., 2020a). Both arginase isoforms have been shown to be expressed in the retina and brain tissues (Caldwell et al., 2018). A1 is widely used as a marker for M2-like reparative microglia/macrophages in CNS studies. Expression of A1 in these cells correlates with better outcomes in stroke models (Hamzei Taj et al., 2016). Despite this, the direct action of A1 in models of stroke has not been studied to our knowledge and this is a first report of the neuroprotective effect of A1 administration. A recent study showed that A1 is expressed by macrophages rather than microglia after permanent middle cerebral artery occlusion (Zarruk et al., 2018). Similarly, A1 has been shown to be upregulated in macrophages but not microglia after traumatic brain injury (TBI) (Hsieh et al., 2013). On the other hand, a recent study used bone marrow chimera to show that A1 is expressed in both microglia and macrophage after ischemic stroke (Cai et al., 2019). One study showed improvement of cerebral ischemia outcomes with the indirect arginase inhibitors, L-citrulline, L-ornithine and L-norvaline (Barakat et al., 2018). However, these amino acids have actions beyond arginase inhibition. We here also report neuroprotection with PEG-A1 treatment against traumatic optic neuropathy. This is in line with a previous report that showed neuroprotection against TBI with A1 overexpression in brain neurons (Madan et al., 2018).

Lipophilic drugs of molecular weight less than 500 Da can readily cross the blood-brain and blood-retina barriers (Pardridge, 2012; Del Amo et al., 2017). PEG-A1 is a hydrophilic drug. The recombinant A1 (37 kDa) enzyme is linked to multiple PEG (5 kDa) molecules and migrates on SDS-PAGE as a 220 kDa band (Lam et al., 2019). PEG-A1 was previously reported to exhibit poor CNS penetration (De Santo et al., 2018). Here we report limited PEG-A1 penetration into the sham retinas or brains after i.p. administration while the penetration is greatly enhanced with IR-injury or cerebral ischemia and breakdown of the blood-retina and blood-brain barriers. These findings support the

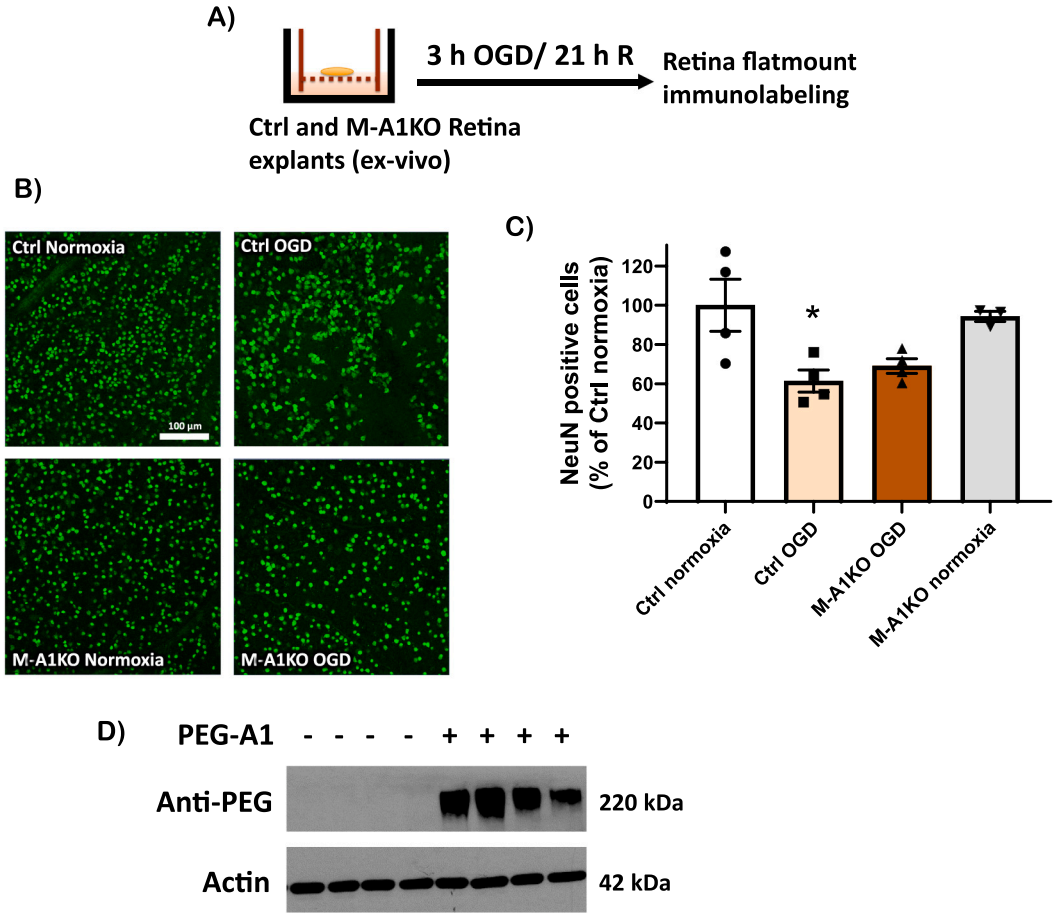

Fig. 7. Explants from control and myeloid A1 KO mice show no difference in neuronal cell death after OGD/R. A) Schematic representation of the experimental protocol for figs. B and C. B, C) Exposing retina explants from Ctrl and M-A1KO mice to OGD/R ex vivo showed similar neuronal degeneration, $n = 3–4$, *$p < 0.05$ vs normoxia. D) Western blotting on primary mouse macrophages shows a strong band for anti-PEG in cells treated with PEG-A1 for 18 h suggesting possible uptake of the drug into the cells.

beneficial effects of systemic administration of PEG-A1 in acute and chronic ischemic injury conditions where the blood-retina or blood-brain barriers are compromised or disrupted. Furthermore, we show PEG-A1 uptake by macrophages in vitro. Our data are in accordance with reports that pegylated proteins can be internalized by macrophages possibly via pinocytosis (Yu et al., 2004; Kelley et al., 2018). However, we were not able to confirm the uptake of PEG-A1 by microglia / macrophages in vivo. It is possible that PEG-A1 affects microglia/ macrophage polarization by depleting L-arginine in the local milieu. Alternatively, the PEG may have been degraded in the period following the PEG-A1 uptake.

We previously showed that intravitreal A1 treatment improves neuronal survival in WT mice after retinal I/R injury. This intravitreal injection was performed using A1 prepared in our lab. In the current study, we obtained and used a pharmaceutical grade of PEG-A1 that is being tested in clinical trials. The mechanism of A1 protection is likely multifaceted. PEG-A1 leads to polyamine accumulation by converting arginine to ornithine, which is further catabolized to polyamines (Brunner et al., 2020). Polyamines have been shown to be neuroprotective in acute retina and brain injury models (Noro et al., 2015a; Noro et al., 2015b; Gilad and Gilad, 1989; Clarkson et al., 2004). While we have not measured polyamine levels in our models, herein we found a reduction in inflammatory cytokines and increase in the neurotrophic factor BDNF with PEG-A1 treatment after ONC. BDNF is known to promote retinal ganglion cell survival and axonal regeneration (Chen and Weber, 2001; Osborne et al., 2018). Interestingly, systemic PEG-A1 treatment did not affect endogenous A1 mRNA levels. This suggests that the mechanism of action of PEG-A1 systemic treatment is independent of endogenous A1 levels.

We also report a reduction in the number of microglia/macrophages after injury which suggests that the neuroprotective action of A1 can be indirect through modulating microglia/macrophages. In line with this, we have previously shown that myeloid specific A1 deletion using the LysM cre promoter, or global hemizygous deletion worsen the retinal IR-injury outcome (Fouda et al., 2018b). Data from our lab and others show LysM cre to be expressed mainly in macrophages, a small subset of microglia and a small percentage of CNS neurons (Fouda et al., 2020b; Orthgiess et al., 2016). In order to confirm that our previous in vivo findings of worsened outcomes in mutant LysM cre-A1 floxed mice subjected to retinal IR injury are indeed due to myeloid cell-specific deletion of A1 and not due to its neuronal deletion, we subjected retina explants from control and LysM cre-A1 floxed mice to oxygen-glucose deprivation / reoxygenation injury. Unlike our previous in vivo data that showed worsened outcome in the myeloid-specific A1 KO retinas, the ex vivo data showed no difference between the control and KO explants after OGD / R. This suggests that the in vivo phenotype seen in our previous study was indeed due to deletion of A1 in infiltrating myeloid cells and not off-target deletion in the neurons. Our future studies will examine the role of A1 in microglia using specific cre promoters such as CXCR1-cre mice.

Our ex vivo retina explant model is unique in providing the opportunity to test neuroprotective agents without involvement of systemic immune cells. We show neuroprotection with PEG-A1 treatment ex vivo, which could be due to a direct protective effect on neurons or to an indirect effect on retinal glia. Interestingly, treatment with PEG-A1 in vitro did not show neuroprotection in two retina neuron cultures (primary mixed neurons and R28 cell line). A previous report showed a protective role of A1 overexpression in motor neurons against trophic factor deprivation in vitro (Estévez et al., 2006). However, our approach using PEG-A1 can lead to L-arginine depletion under in vitro conditions. L-arginine is a semi-essential amino acid in vivo, yet it is a required supplement in cell cultures (Morgan et al., 1958). Furthermore, L-arginine supplementation has been shown to provide neuroprotection via preservation of arginase activity and formation of polyamines in motor neurons (Lee et al., 2009). Our future studies will delineate the effect of PEG-A1 on polyamine levels in vivo, and myeloid cell recruitment and activation in retina and brain injury models.

In conclusion, systemic treatment with PEG-A1 post-injury crosses the blood-retina and blood-brain barriers and provides neuroprotection in retinal IR injury, TON and stroke mouse models. This approach may offer a new therapy for acute retina and brain injury.

Authors' contribution

AYF: design and performance of experiments involving retinal IR, ONC and explant models as well as in vitro neuron cultures, and drafting the manuscript. WE: design and performance of experiments involving the stroke model and editing the manuscript. ZX: helped with the ONC model, TL and ES: helped with the neuron cultures and western blotting. SAHZ and AAA helped with qPCR experiments. SPN: provided reagents and guidance on the neuron cultures experiments. PC: provided the PEG-A1 and advised on its use and dosing. RWC: provided supervision and guidance with the stroke model study and edited the final manuscript. RBC: conceived and supervised the project, provided critical feedback and revised the final manuscript.

Declaration of Competing Interest

AF, RBC, and RWC have a pending patent on the use of arginase 1 as a treatment for ischemic retinopathies. PNMC is the chief executive officer of Bio-Cancer Treatment International Limited and holds stocks or shares in Bio-Cancer Treatment International Limited. The other authors declare no conflict of interest.

Acknowledgments

This work was supported by grants from the National Institute of Health (NIH grant R01-EY11766 to RBC, RWC), the Department of Veterans Affairs, Veterans Health Administration (RBC), Office of Research and Development, Biomedical Laboratory Research and Development (BX001233 to RBC), K99 award (1K99EY029373-01A1 to AYF) and the Culver Vision Discovery Institute at Augusta University. The research reported in this publication was also supported by the NIH core grant number P30EY031631. The content is solely the responsibility of the authors and does not necessarily represent the official views of the NIH. R. B. Caldwell is the recipient of a Research Career Scientist Award from the Department of Veterans Affairs. The contents do not represent the views of the Department of Veterans Affairs or the United States Government. The funders had no role in study design, data collection and analysis, decision to publish, or preparation of the manuscript. The authors would like to thank Dr. Tauheed Ishrat at the University of Tennessee Health Science Center (UTHSC) for his help with standardizing the mouse MCAO model.

Appendix A. Supplementary data

Supplementary data to this article can be found online at https://doi.org/10.1016/j.expneurol.2021.113923.

References

Alarautalahti, V., Ragauskas, S., Hakkarainen, J.J., Uusitalo-Järvinen, H., Uusitalo, H., Hyttinen, J., et al., 2019. Viability of mouse retinal explant cultures assessed by preservation of functionality and morphology. Invest. Ophthalmol. Vis. Sci. 60, 1914–1927.

Barakat, W., Fahmy, A., Askar, M., El-Kannishy, S., 2018. Effectiveness of arginase inhibitors against experimentally induced stroke. Naunyn Schmiedeberg's Arch. Pharmacol. 391, 603–612.

Bieber, M., Gronewold, J., Scharf, A.C., Schuhmann, M.K., Langhauser, F., Hopp, S., et al., 2019. Validity and reliability of neurological scores in mice exposed to middle cerebral artery occlusion. Stroke. 50, 2875–2882.

Brunner, J.S., Vulliard, L., Hofmann, M., Kieler, M., Lercher, A., Vogel, A., et al., 2020. Environmental arginine controls multinuclear giant cell metabolism and formation. Nat. Commun. 11, 431.

Cai, W., Dai, X., Chen, J., Zhao, J., Xu, M., Zhang, L., et al., 2019. Stat6/arg1 promotes microglia/macrophage efferocytosis and inflammation resolution in stroke mice. JCI Insight. 4.
Caldwell, R.W., Rodriguez, P.C., Toque, H.A., Narayanan, S.P., Caldwell, R.B., 2018. Arginase: a multifaceted enzyme important in health and disease. Physiol. Rev. 98, 641–665.
Chen, H., Weber, A.J., 2001. Bdnf enhances retinal ganglion cell survival in cats with optic nerve damage. Invest. Ophthalmol. Vis. Sci. 42, 966–974.
Cheng, P.N., Lam, T.L., Lam, W.M., Tsui, S.M., Cheng, A.W., Lo, W.H., et al., 2007. Pegylated recombinant human arginase (rharg-peg5,000mw) inhibits the in vitro and in vivo proliferation of human hepatocellular carcinoma through arginine depletion. Cancer Res. 67, 309–317.
Clarkson, A.N., Liu, H., Pearson, L., Kapoor, M., Harrison, J.C., Sammut, I.A., et al., 2004. Neuroprotective effects of spermine following hypoxic-ischemic-induced brain damage: a mechanistic study. FASEB J. 18, 1114–1116.
De Santo, C., Booth, S., Vardon, A., Cousins, A., Tubb, V., Perry, T., et al., 2018. The arginine metabolome in acute lymphoblastic leukemia can be targeted by the pegylated-recombinant arginase i bct-100. Int. J. Cancer 142, 1490–1502.
Del Amo, E.M., Rimpelä, A.K., Heikkinen, E., Kari, O.K., Ramsay, E., Lajunen, T., et al., 2017. Pharmacokinetic aspects of retinal drug delivery. Prog. Retin. Eye Res. 57, 134–185.
Eldahshan, W., Ishrat, T., Pillai, B., Sayed, M.A., Alwhaibi, A., Fouda, A.Y., et al., 2019. Angiotensin ii type 2 receptor stimulation with compound 21 improves neurological function after stroke in female rats: a pilot study. Am. J. Physiol. Heart Circ. Physiol. 316, H1192–h1201.
Estévez, A.G., Sahawneh, M.A., Lange, P.S., Bae, N., Egea, M., Ratan, R.R., 2006. Arginase 1 regulation of nitric oxide production is key to survival of trophic factor-deprived motor neurons. J. Neurosci. 26, 8512–8516.
Feun, L.G., Kuo, M.T., Savaraj, N., 2015. Arginine deprivation in cancer therapy. Curr. Opin. Clin. Nutr. Metab. Care. 18, 78–82.
Fouda, A.Y., Xu, Z., Shosha, E., Lemtalsi, T., Chen, J., Toque, H.A., et al., 2018a. Arginase 1 promotes retinal neurovascular protection from ischemia through suppression of macrophage inflammatory responses. Cell Death Dis. 9, 1001.
Fouda, A.Y., Xu, Z., Shosha, E., Lemtalsi, T., Chen, J., Toque, H.A., et al., 2018b. Arginase 1 promotes retinal neurovascular protection from ischemia through suppression of macrophage inflammatory responses. Cell Death Dis. 9, 1001.
Fouda, A.Y., Eldahshan, W., Narayanan, S.P., Caldwell, R.W., Caldwell, R.B., 2020a. Arginase pathway in acute retina and brain injury: therapeutic opportunities and unexplored avenues. Front. Pharmacol. 11, 277.
Fouda, A.Y., Xu, Z., Narayanan, S.P., Caldwell, R.W., Caldwell, R.B., 2020b. Utility of lysm-cre and cdh5-cre driver mice in retinal and brain research: an imaging study using tdtomato reporter mouse. Invest. Ophthalmol. Vis. Sci. 61, 51.
Gilad, G.M., Gilad, V.H., 1989. Treatment with polyamines can prevent monosodium glutamate neurotoxicity in the rat retina. Life Sci. 44, 1963–1969.
Hamzei Taj, S., Kho, W., Riou, A., Wiedermann, D., Hoehn, M., 2016. Mirna-124 induces neuroprotection and functional improvement after focal cerebral ischemia. Biomaterials. 91, 151–165.
Han, G., Casson, R.J., Chidlow, G., Wood, J.P.M., 2014. The mitochondrial complex i inhibitor rotenone induces endoplasmic reticulum stress and activation of gsk-3β in cultured rat retinal cells. Invest. Ophthalmol. Vis. Sci. 55, 5616–5628.
Hernandez, C.P., Morrow, K., Lopez-Barcons, L.A., Zabaleta, J., Sierra, R., Velasco, C., et al., 2010. Pegylated arginase i: a potential therapeutic approach in t-all. Blood. 115, 5214–5221.
Hsieh, C.L., Kim, C.C., Ryba, B.E., Niemi, E.C., Bando, J.K., Locksley, R.M., et al., 2013. Traumatic brain injury induces macrophage subsets in the brain. Eur. J. Immunol. 43, 2010–2022.
Jindal, V., 2015. Interconnection between brain and retinal neurodegenerations. Mol. Neurobiol. 51, 885–892.
Jittiporn, K., Suwanpradid, J., Patel, C., Rojas, M., Thirawarapan, S., Moongkarndi, P., et al., 2014. Anti-angiogenic actions of the mangosteen polyphenolic xanthone derivative α-mangostin. Microvasc. Res. 93, 72–79.
Johnson, T.V., Martin, K.R., 2008. Development and characterization of an adult retinal explant organotypic tissue culture system as an in vitro intraocular stem cell transplantation model. Invest. Ophthalmol. Vis. Sci. 49, 3503–3512.
Kelley, W.J., Fromen, C.A., Lopez-Cazares, G., Eniola-Adefeso, O., 2018. Pegylation of model drug carriers enhances phagocytosis by primary human neutrophils. Acta Biomater. 79, 283–293.
Kong, D., Gong, L., Arnold, E., Shanmugam, S., Fort, P.E., Gardner, T.W., et al., 2016. Insulin-like growth factor 1 rescues r28 retinal neurons from apoptotic death through erk-mediated bimel phosphorylation independent of akt. Exp. Eye Res. 151, 82–95.
Lam, S.K., Yan, S., Xu, S., U KP, Cheng PN, Ho JC., 2019. Endogenous arginase 2 as a potential biomarker for pegylated arginase 1 treatment in xenograft models of squamous cell lung carcinoma. Oncogenesis. 8, 18.
Lee, J., Ryu, H., Kowall, N.W., 2009. Motor neuronal protection by l-arginine prolongs survival of mutant sod1 (g93a) als mice. Biochem. Biophys. Res. Commun. 384, 524–529.
London, A., Benhar, I., Schwartz, M., 2013. The retina as a window to the brain—from eye research to cns disorders. Nat. Rev. Neurol. 9, 44–53.
Madan, S., Kron, B., Jin, Z., Al Shamy, G., Campeau, P.M., Sun, Q., et al., 2018. Arginase overexpression in neurons and its effect on traumatic brain injury. Mol. Genet. Metab. 125, 112–117.
Mathew, B., Ravindran, S., Liu, X., Torres, L., Chennakesavalu, M., Huang, C.C., et al., 2019. Mesenchymal stem cell-derived extracellular vesicles and retinal ischemia-reperfusion. Biomaterials. 197, 146–160.
McLaughlin, T., Dhimal, N., Li, J., Wang, J.J., Zhang, S.X., 2018. P58(ipk) is an endogenous neuroprotectant for retinal ganglion cells. Front. Aging Neurosci. 10, 267.
Morgan, J.F., Morton, H.J., Pasieka, A.E., 1958. The arginine requirement of tissue cultures. I. Interrelationships between arginine and related compounds. J. Biol. Chem. 233, 664–667.
Morrow, K., Hernandez, C.P., Raber, P., Del Valle, L., Wilk, A.M., Majumdar, S., et al., 2013. Anti-leukemic mechanisms of pegylated arginase i in acute lymphoblastic t-cell leukemia. Leukemia. 27, 569–577.
Noro, T., Namekata, K., Kimura, A., Guo, X., Azuchi, Y., Harada, C., et al., 2015a. Spermidine promotes retinal ganglion cell survival and optic nerve regeneration in adult mice following optic nerve injury. Cell Death Dis. 6, e1720.
Noro, T., Namekata, K., Azuchi, Y., Kimura, A., Guo, X., Harada, C., et al., 2015b. Spermidine ameliorates neurodegeneration in a mouse model of normal tension glaucoma. Invest. Ophthalmol. Vis. Sci. 56, 5012–5019.
Orthgiess, J., Gericke, M., Immig, K., Schulz, A., Hirrlinger, J., Bechmann, I., et al., 2016. Neurons exhibit lyz2 promoter activity in vivo: implications for using lysm-cre mice in myeloid cell research. Eur. J. Immunol. 46, 1529–1532.
Osborne, A., Khatib, T.Z., Songra, L., Barber, A.C., Hall, K., Kong, G.Y.X., et al., 2018. Neuroprotection of retinal ganglion cells by a novel gene therapy construct that achieves sustained enhancement of brain-derived neurotrophic factor/tropomyosin-related kinase receptor-b signaling. Cell Death Dis. 9 (1007–1007).
Pardridge, W.M., 2012. Drug transport across the blood-brain barrier. J. Cereb. Blood Flow Metab. 32, 1959–1972.
Perígolo-Vicente, R., Ritt, K., Gonçalves-de-Albuquerque, C.F., Castro-Faria-Neto, H.C., Paes-de-Carvalho, R., Giestal-de-Araujo, E., 2014. Il-6, a1 and a2ar: a crosstalk that modulates bdnf and induces neuroprotection. Biochem. Biophys. Res. Commun. 449, 477–482.
Shosha, E., Xu, Z., Yokota, H., Saul, A., Rojas, M., Caldwell, R.W., et al., 2016. Arginase 2 promotes neurovascular degeneration during ischemia/reperfusion injury. Cell Death Dis. 7 (e2483-e2483).
Xu, Z., Fouda, A.Y., Lemtalsi, T., Shosha, E., Rojas, M., Liu, F., et al., 2018. Retinal neuroprotection from optic nerve trauma by deletion of arginase 2. Front. Neurosci. 12, 970.
Yau, T., Cheng, P.N., Chan, P., Chen, L., Yuen, J., Pang, R., et al., 2015. Preliminary efficacy, safety, pharmacokinetics, pharmacodynamics and quality of life study of pegylated recombinant human arginase 1 in patients with advanced hepatocellular carcinoma. Investig. New Drugs 33, 496–504.
Yu, D., Zhao, Y., Choe, Y.H., Zhao, Q., Hsieh, M.-C., Peng, P., 2004. Cellular penetration and localization of polyethylene glycol. Cancer Res. 64 (149–149).
Zarruk, J.G., Greenhalgh, A.D., David, S., 2018. Microglia and macrophages differ in their inflammatory profile after permanent brain ischemia. Exp. Neurol. 301, 120–132.